International Journal of Chemical and Biochemical Sciences
(ISSN 2226-9614)

Journal Home page:www.iscientific.org/Journal.html

Kinetic and electrochemical corrosion inspection of carbon steel X70 in 1M HCl solution by *Senecio hoggariensis* extract as an eco-friendly inhibitor

Ibtissem Bellaoueur[a]*, Messaouda Allaoui[b], Ali Lounas[a], Oumelkheir Rahim[b], Noureddine Gherraf[c] and Brahim Labed[d]

*[a]*University Kasdi Merbah, Faculty of mathematics and Matter sciences, Chemistry Department, Laboratory of Valuation and Promotion for Saharan Resources, Ghardaia Road, Ouargla, Algeria, [b]University Kasdi Merbah, Faculty of mathematics and Matter sciences, Chemistry Department, Electrochemical Laboratory, Ghardaia Road, Ouargla, Algeria, [c]Laboratory of Natural Resources and Management of Sensitive Environments, Larbi ben M'hidi university, Oum El Bouaghi, 04000, Algeria and [d]Superior Normal School, Ouargla, Algeria*

Abstract

The inhibitory capacity of the *Senecio hoggariensis* extract was studied on the corrosion of carbon steel X70 in 1 M hydrochloric acid medium through weight loss and electrochemical ways. The results obtained from the weight loss method clarified that the increased concentration of the plant extract improved the inhibitory action up to a maximum rate of 95.23 % at 12. 5% (v/v) of the inhibitor. We also studied the impact of temperature on the corrosion with non-attendance and attendance of the optimum concentration in temperature range from 290 to 350 K and computed the activation energy, enthalpy, and entropy. The study of the Tafel curves showed that our green inhibitor bottled-up the corrosion processes of steel X70 in hydrochloric acid and acted as a cathodic type inhibitor. Impedance data also indicated that adsorption of the extract on the metal surface afforded protection from corrosion in the acidic solution. The adsorption isotherm was found to follow the Langmuir model.

Keywords: *Senecio hoggariensis*; Carbon steel; Corrosion inhibitor; Tafel; Impedance

Full length article **Corresponding Author*, e-mail:ibtissem.bellaoueur@yahoo.com

1. Introduction

Iron and its alloys are used in many industrial applications of acids, such as oil extraction, crude oil refining, and petrochemical fittings. These industries require different processes, such as acid pickling, industrial cleaning, acid expansion, and regular intervals that improve the productivity of industrial processes and stronger solutions using hydrochloric acid [1-2]. Corrosion destroys alloy and metal components, resulting in many structural losses such as tides and repairs [3]. To minimize corrosion losses, many different methods are used, such as material recovery, mixing of production fluids and control of chemical inhibition [3-4]. To avoid damaging metal surfaces in corrosive environments, inhibitors have been used as the best way to lower corrosion [5]. To protect metals from corrosion, many organic and inorganic compounds have been used owing to the presence of π electrons, polar functions with their S, O or N atoms and heterocyclic compounds. The adsorption of these compounds in the area of the metal causes the closure of its active sites and thus reduces the rate of corrosion. Most inhibitors are highly active against corrosion, but they affect humans and environment since they are not biodegradable and expensive [6].

Currently, plant extracts are used as alternative inhibitors of synthetic compounds containing many oxygen-containing compounds in addition to sulfur and nitrogen. They are of ecological nature, non-hazardous, inexpensive and renewable [7]. Various plant extracts have demonstrated their inhibitory ability against metals and alloys corrosion such as *Parthenium hystophrous L* [8], *Zygophyllum album* [9], Henna leaves (*Lawsonia inermis L*) [10], *Kopsia singapurensis* [11], *Nypa fruticans wurmb* [12] and *Opuntia ficus indica* [13]. The objective of this study is to estimate the effect of *Senecio hoggariensis* extract on the corrosion of X70 carbon steel in a 1 M HCl solution by weight loss and electrochemical studies.

2. Experimental

2.1. Sample preparation

The sample used in this study is X70 carbon steel and its chemical ingredients are noted in Table 1. The carbon steel sample was cut into two shapes, one which parallels of rectangles with a size of 1.2 × 1.1 × 0.75 cm and was used in the weight loss method and the other was used as a working electrode in the electrochemical methods and it is surface roof tested 1 cm^2. Before each corrosion test, the samples were mechanically polished with an emery paper of different grades (150, 320, 400, 600, 800 and 1200), then washed with distilled water then dehydrated at room temperature of 15 ˚C.

2.2. Inhibitor making

Senecio hoggariensis (SH) plant was collected in February 2017 in the region of Tamanrasset (Algeria). The aerial part of the plant was dried in shade and stored in paper bags away from light and moisture. 100 g of dry powder was steeped in a 1 M hydrochloric acid solution for 24 hours. After a full day, the acid solution was filtered, the filtrate collected and maintained until used.

2.3. Phytochemical screening

To determine and limit the different active substances present in SH extract, we performed many preliminary phytochemical tests [14, 15].

2.4. Solutions preparation

The electrolyte of corrosive medium (1M HCl) was prepared by dilution of analytical reagent grade 37 % HCl with distilled water. The stock solution of SH extract was used to prepare different concentrations that changed as follows: 0.25 %, 0.62 %, 1.25 %, 3.75 %, 6.25 % and 12.5 % (v/v).

2.5. Weight loss study

In weight loss studies, steel X70 specimens with dimensions 1.2 × 1.1 × 0.75 cm were tested in non-attendance and attendance of different concentrations prepared from plant extracts in 1 M HCl. The volume of the solution used for every test was 100 ml and the required immersion time was 60 minutes. The sample was weighed by an electronic balance before and after immersion. Then, it was washed with distilled water and dried before being re-weighed.

The surface coverage (θ), inhibition efficiency (*EI* %) and corrosion rate (*Cr*) were calculated from the following equations [16]:

$$\theta = \frac{(W_0 - W_i)}{W_0} \dots (1)$$

$$EI\% = \frac{(W_0 - W_i)}{W_0}.100 \dots (2)$$

W_i and W_0 are the weight loss values in non-attendance and attendance of inhibitor, respectively.

$$Cr\ (mm/y) = \frac{87.6 \times W}{StD} \dots (3)$$

Where, *W* is a weight loss of carbon steel (mg), S the size of the piece (cm^2), *t* is the exposition time (h) and D the density of steel ($g.cm^{-3}$).

2.6. Electrochemical tests

Electrochemical measurements were performed using a personal computer-driven Volta lab 40 model PGZ301 Potentiostat/Galvano station equipped with VoltaMaster 4 software. A typical three electrodes cell with a working electrode made of carbon steel X70. The auxiliary electrode was a platinum plate ($1cm^2$) and the reference electrode was represented by a saturated calomel electrode (SCE). Polarization curves were taken with the scan speed of 0.5 $mV.s^{-1}$, in the potential range of -750 mV to -200 mV. The immersion time of the X70 plates in the blank as well as in the existence of various concentrations of SH extract was 40 minutes in open circuit at room temperature of 26 ˚C.

We obtained the inhibition efficiency (*IE* %) through the Tafel curves according to the following equation:

$$IE\% = \left(1 - \frac{i_{corr}}{i^{\circ}_{corr}}\right).100 \dots (4)$$

Where i°_{corr}, i_{corr} is the corrosion current density in non-attendance and attendance of the inhibitor, respectively.

Electrochemical impedance spectroscopy (EIS) measurements were taken after 30 minutes of immersion time of the carbon steel plates in corrosive media, at the corrosion potential of -493 mV (E_{corr}), in a frequency range from 100 KHz to 10 mHz by a parturition signal of 10mV amplitude peak to peak, at room temperature 26 ˚C [17, 18].

R_{ct} was used to calculate the *IE*%, according to the equation:

$$IERct\% = 1 - \frac{R^{\circ}_{ct}}{R_{ct}}.100 \dots (5)$$

R°_{ct}, R_{ct} is the charge transfer resistances of metal in non-attendance and attendance of plant extract, respectively.

3. Results and discussion

3.1. Characteristics of inhibitors and their effect on inhibition of corrosion

The role of inhibitors is to form a single layer or several molecular layers against the aggression of the acidic solution. This depends on the phytochemical compounds that are present at different rates from one organ to another at the plant level as well as its geographical position [19]. The inhibitory characteristics of these compounds are derived from the adsorption capacity of their molecules, where the polar group acts as a reaction center for the adsorption operation [20]. The photochemical screening studies of SH extract are shown in Table 2. The results obtained showed that the SH extract contains alkaloids, tannins, flavonoids, terpenoids, saponosides, resins, glycosides, and phenols. This confirms that the efficiency of

inhibition is due to the existence of metabolites that have many functional groups.

3.2. Weight loss method

3.2.1. Effect of concentration

The method of weight loss found wide practical applications. The main feature of this way is its relative simplicity [21,22]. The weight loss measurements for the corrosion of carbon steel in the solution of HCl including various concentrations of SH extract were shown in Figure 1 and Table 3. The results in Table 3 showed that the inhibitor reduced the corrosion rate of carbon steel. It was remarked that by raising the concentration of the plant extract, the corrosion rate decreased, while the inhibition efficiency (*IE* %) and surface coverage (θ) increased. The inhibition efficiency reached a maximum value of 95.23 % at 12.5% (v/v) of plant extract. The addition of plant extracts in the acid medium raises the performance of inhibition. This proves that the chemical constituent of these extract was adsorbed on the surface of the metal, resulting in the covering the reaction sites [22].

3.2.2. Effect of temperature

To study of the impact of temperature on the corrosion speed and the inhibition efficiency of SH extract was conducted. The weight loss measurements were made at a temperature between 290 and 350 K in non-attendance and attendance of the inhibitor at 12.5% (V/V) for one hour. The results are exposed in Figure 2 and Table 4. The results in Table 4 show that the higher the temperature, the higher the corrosion speed and the lower the inhibition efficiency. It can be said that the reduction in the inhibition efficiency with high temperature is due to increased adsorption of inhibitor particles in the surface of the steel [23].

3.2.3. Kinetic and thermodynamic parameters for the inhibition operation

Activation energies of corrosion operation in non-attendance and attendance of the green eco-friendly were computed depending on the Arrhenius equation:

$$\mathrm{Cr} = \mathrm{Aexp}^{-\mathrm{Ea/RT}} \dots (6)$$

Where A is Arrhenius Pre-exponential factor, *R* is a universal gas constant and *T* is absolute temperature. Linearization of equation (6) gives an equation (7) [24].

$$\mathrm{LnCr} = \mathrm{LnA} - \frac{\mathrm{Ea}}{\mathrm{RT}} \dots (7)$$

A plot of LnCr against $\frac{1}{T}$gives a slope of - $\frac{Ea}{R}$, where activation energy (*Ea*) values are presented in Table 5. Arrhenius diagrams for the corrosion speed of carbon steel in 1M HCl in non-attendance and attendance inhibitor are shown in Figure 3. The calculated activation energy rises with the addition of SH extract compared to a blank (Table 5). This marked rise in activation energy with a increase in temperature may be attributed to the observed reduction in adsorption of the inhibitor on the surface of steel [25]. Furthermore, it was suggested that *Ea* values between 40 to 80kJ.mol^{-1} would be obedient to physical adsorption [26].

Enthalpy of activation (ΔH^*) and entropy of activation (ΔS^*) values were obtained through the linearized transition state theory equation [24]

$$\mathrm{Ln}\left(\frac{\mathrm{Cr}}{\mathrm{T}}\right) = \mathrm{Ln}\left(\frac{\mathrm{R}}{\mathrm{Nh}}\right) + \frac{\Delta \mathrm{S}^*}{\mathrm{R}} - \frac{\Delta \mathrm{H}^*}{\mathrm{RT}} \dots (8)$$

Where *h* is Planck's constant and *N* is Avogadro's number. A plot of $\mathrm{Ln}\left(\frac{Cr}{T}\right)$ versus $\frac{1}{\mathrm{T}}$ will give a straight line and the slope is equal to - $\frac{\Delta H^*}{R}$ and the intercept is $\mathrm{Ln}\left(\frac{R}{Nh}\right) + \frac{\Delta S^*}{R}$, from where values of ΔH^* and ΔS^* were calculated and are presented in Figure 4 and Table 5.

Table 5 shows that enthalpy values in the absence of the inhibitor were lower than those in its presence. The positive values of ΔH^* account for the endothermic nature of the steel degeneracy process, indicating that this process is slow in the existence of inhibitors [27, 28]. Enthalpy of the physical adsorption process is typically less than 80KJ.mol^{-1} while enthalpy of the chemical absorption process is approximate 100KJ.mol^{-1} [29]. The negative value of ΔS^* in existence of the inhibitor shows that the activation complex in the rate-determining step is an association rather than dissociation step, meaning that a diminution in the chaos when moving from the reactant to the activated complex [30].

Also, free energy (ΔG^*) was calculated at different temperatures according to equation (9) and the results recorded in Table 5.

$$\Delta \mathrm{G}^* = \Delta \mathrm{H}^* - \mathrm{T}\Delta \mathrm{S}^* \dots (9)$$

Free energy is a measure of the stability of the activated complex. Therefore, as shown in Table 5, this stability diminished with a rising temperature [31].

3.3. Electrochemical methods

3.3.1. Open circuit potential

Open circuit changes in terms of the time of 1M HCl working electrode with the non-attendance and attendance of inhibitor as plotted in Figure 5. In the case of the blank solution, the steady-state values of OCP were more negative than the immersion potential (Eocp at t = 0). This suggests that before the steady-state condition is achieved, the oxide film formed from the air must dissolve on the electrode before immersion [32]. With the addition of the inhibitor at different concentrations, the steady-state potential of the test electrodes has been converted to more positive values. This denotes the passivation of the alloy [33].

3.3.2. Potentiodynamic polarization

Potentiodynamic polarization curves for carbon steel in 1M HCl including various concentrations of SH extract are shown in Figure 6. The electrochemical kinetic factors such as corrosion potential (E_{corr}), corrosion current density (i_{corr}), cathodic Tafel slope (b_c) and anodic Tafel slope (b_a) are presented in Table 6.

The polarization Tafel curves showed that the anodic and cathodic reactions resulting from the corrosion of the metal in 1M HCl solution were inhibited by adding various concentrations of the plant extract. We observed from Table 6 that the current density diminished with a rising concentration of the SH extract, which proves that the inhibitor molecules were absorbed in the surface of the carbon steel sample. The highest percentage of inhibition was 97.40% at the highest concentration of green inhibitor. We also noticed that the addition of the plant extract changed the values E_{corr} in the cathodic and anodic direction as well, but the change is clear in the cathodic direction. This denotes that the inhibition mechanism was following a cathodic type. An inhibitor can be categorized as either anodic or cathodic if the displacement in the E_{corr} is greater than ± 85 mV compared to the corrosion of the blank solution [34]. Besides, the displacement of the E_{corr} with more than -85 mV at 12.5% (v/v) of plant extract confirms that SH extract acts as a cathodic type inhibitor.

3.3.3. Electrochemical impedance spectroscopy (EIS)

Nyquist diagrams for carbon steel in 1 M HCl solutions in non-attendance and attendance at different concentrations of SH extract is presented in Figure 7. The impedance parameters for carbon steel in 1M HCl solutions in non-attendance and attendance of the inhibitor obtained from the Nyquist plots are listed in Table 7.

The double-layer capacitance (C_{dl}) and the frequency at which the imaginary component of the impedance is maximal $-Z_{im}(max)$ is found and represented using the following equation:

$$C_{dl} = \frac{1}{2\pi R_{ct} f_{max}} \dots (10)$$

We observed through the Nyquist curves (Figure 7) that the half-circle depressant equal to one and the diameter increases with the increased concentration of the inhibitor. This explains that the corrosion of steel is verified by the charge transfer process as well as the surface of the heterogeneous metal due to the roughness of the electrode surface or interfacial effect [35]. Table 7 shows that the charge transfer resistance (R_{ct}) increased from 41.85 to 799.7ohm.cm^2 at the optimum concentration of the inhibitor while the capacitance decreased from 85.18 to 40.63µF.cm^{-2} at the addition of 12.5% (v/v) of plant extract. A decrease in capacitance resulted when adding the SH extract. This may be assigned to the growing thickness of the double layer and/or augmentation of the local dielectric constant [36]. This indicates that the inhibitor works by adsorption at the interface of the metal/solution and that the decrease in C_{dl} values is due to the gradual replacement of the water molecules by adsorbing the inhibitor molecules on the electrode surface, thereby reducing the extent of the metal degradation [37]. The impedance data were analyzed by an electrical equivalent circuit consisting of the solution resistance (R_s), R_{ct} and C_{dl} as illustrated in Figure 8.

Bode and phase angle plots of carbon steel in 1M HCl in non-attendance and attendance at different concentrations of SH extract are shown in Figure 9. These plots show that log |Z| and the phase angle increases in the high-frequency region, and this increase was associated with the increased concentration of plant extract. However, in the presence of the blank, the phase angle is small due to the corrosion of the surface of the working electrode by hydrochloric acid which makes it irregular. The single narrow peaks in the phase-angle diagrams (Figure 9b) indicate a one-time stability of the corrosion process in the metal-solution interface in both cases [38]. Raising the roughness of the metal roof in the existence of the inhibitor diminished the phase angle in the corrosion process. While the addition of the SH extract resulted from the homogeneity of the surface and this led to an increase in the phase angle [34].

3.4. Adsorption isotherm

The adsorption inhibitor process depends on its electronic properties, the nature of the metal surface, the temperature, the steric effects and varying degrees of movement of the roof sites. The water molecules could also be adsorbed at the metal/solution interface. In the aqueous solution, the inhibitor molecules act as an alternative to the H_2O molecules on the surface of the electrode [39].

$$Org_{(sol)} + xH_2O_{(ads)} \leftrightarrow xH_2O_{(sol)} + Org_{(ads)} \dots (11)$$

X is the size ratio, that is, the number of water molecules replaced by one organic inhibitor.

The preceding equation explained that the power of the interaction among the metal and the inhibitor should be greater than the strength of the interaction between the metal and water molecules. To understand adsorption processes using adsorption temperature. Langmuir adsorption isotherm explains whether the adsorption phenomenon is physical or chemical, while Temkin adsorption isotherm explains the heterogeneity formed on the surface of the metal. The chemical adsorption is attributed to Temkin isotherm [40]. To identify the method of adsorption of chemical constituents of plant extract on the surface of steel X70, experimental data were tested with several isothermal adsorptions, including Langmuir, Frumkin, and Temkin.

$$\text{Langmuir:} \frac{C}{\theta} = \frac{1}{K} + aC \dots (12)$$

$$\text{Temkin: } \log\frac{\theta}{C} = \log K - g\theta \dots (13)$$

$$\text{Frumkin: } \log\left[\frac{\theta}{(1-\theta)C}\right] = \log K + g\theta \dots (14)$$

Where θ the surface coverage, k is the adsorption equilibrium constant, *C* is the concentration of inhibitor, "a" and "g" are the adsorbate factors.

The data obtained in the Langmuir, Temkin and Frumkin isotherms of three methods, which are based on the correlation coefficient R^2 resulting from the plot of the surface coverage against the concentration of the adsorbate, are shown in Figures 10, 11, 12 and Table 8.

The linear relationship between (C/θ) and (C) is represented in Figures 10a, 11a, and 12a. The factors of Langmuir isotherm are shown in Table 8. The ideal Langmuir isotherm plot should have a slope equal to the unit and the intercept is close to zero [41]. The tendencies of Langmuir curves here was close to the unit and the intercepts were zero, and correlation coefficients (0.998, 0.999 and 0.999) were close to 1, which confirms that the Langmuir isotherm was appropriate for the adsorption behavior of SH extract [42].

Temkin isotherm is considered to be one of the properties of the chemical adsorption and monolayer, in addition to its reference to the interaction of uncharged particles on a heterogeneous roof [43]. Figure 10b, Figure 11b, and Figure 12b shows the linear relationship between log (θ/C) and (θ) for Temkin adsorption isotherm, where the adsorption factors are taken are shown in Table 8, which indicates the positive values of "g". This shows that there is an act of attraction in the adsorbent layer. However, in the current study, we found that this adsorption property of physical adsorption and this is confirmed by a decrease in IE% despite the increase in temperature [42].

Frumkin isotherm is expanded to Langmuir isotherm [46]. It takes into account the possibility of interaction between the adsorbent species and the range of minerals, by attraction or repulsion [44]. Figure 10c, Figure 11c, and Figure 12c show the linear relationship between log (θ/ (1- θ) C) and (θ) for Frumkin adsorption isotherm and the adsorption parameters obtained are recorded in Table 8. The value of the adsorption factor "g" is positive and it explains the attractive action of the inhibitor on the surface of the electrode [45]. However, in this adsorption, the parameter "g" was negative, indicating the repulsion behavior of inhibitor on the roof of carbon steel.

Table 1. Table of chemical elements of carbon steel X70.

Elements	C	P	S	Si	Mn	Cr	Ni	Cu	Al	Nb	V	Ti	Mo	Fe
wt.10^{-3}	65	2	1	245	1685	42	26	10	42	67	14	19	5	Residual

Table 2. The phytochemical checking studies of SH extract.

Tests	Alkaloids	Tannins	Flavonoids	Terpenoids	Saponosides	Resins	Phenols	Glycosides
Results	(+)	(+)	(+)	(+)	(+)	(+)	(+)	(+)

Table 3. Corrosion factors for the steel in 1M HCl containing various concentrations of SH extract.

C% (v/v)	*Cr* (mm/y)	*EI* %	$\boldsymbol{\theta}$
Blank	4.137	----	----
0.25	1.571	62.02	0.620
1.25	1.115	73.04	0.730
3.75	0.590	85.73	0.857
6.25	0.394	90.46	0.904
12.5	0.197	95.23	0.952

Table 4. The action of temperature on corrosion speed and the inhibition efficacy of carbon steel in 1M HCl in non-attendance and attendance of 12.5% (v/v) of inhibitor**.**

***T* (K)**	***Cr*$_0$ (mm/y)**	***Cr*$_{inh}$ (mm/y)**	***EI* %**
290	5.078	0.262	94.82
311	14.91	1.325	91.11
330	75.67	4.579	93.94
350	330.2	26.00	92.12

Table 5. Activation parameters of the dissolution of carbon steel in 1M HCl in non-attendance and attendance optimum concentration inhibitor.

	Ea(kJ.mol^{-1})	ΔH^*(kJ.mol^{-1})	ΔS^*(J.mol^{-1}.K^{-1})	ΔG^*(KJ.mol^{-1})			
				290	311	330	350
Blank	59.45	56.81	-37.16	67.59	68.37	69.08	69.82
12.5% (v/v) of SH	63.44	60.80	-46.93	74.42	75.40	76.29	77.23

extract							

Table 6. Potentiodynamic polarization factors for the corrosion of carbon steel in 1M HCl solution including various concentrations of inhibitor.

C%(V/V)	*Rp* (ohm.cm^2)	E_{corr}(mV)	i_{corr} (mA/cm^2)	β_a (mV)	β_c (mV)	*IE*%
Blank	43.75	-493.4	1.005	131.7	-163	----
0.25	108.9	-509.2	0.277	113	-130	72.37
0.62	209.7	-485.2	0.190	208	-232.8	81.05
3.75	211.8	-611.1	0.101	275.7	-98.7	89.91
6.25	202.1	-607	0.036	170.2	-78.2	96.39
12.5	213.5	-629	0.026	170.9	-69.2	97.40

Table 7. The impedance parameters for carbon steel in 1M HCl solutions in non-attendance and attendance of the inhibitor.

C%(V/V)	R_{ct}(ohm.cm^2)	C_{dl}(µF/cm^2)	f_{max}(Hz)	IE_{Rct}%
Blank	41.85	85.18	44.66	….
0.25	116.6	68.22	20.01	64.10
0.62	176	57.13	15.83	76.22
3.75	432.8	46.33	7.941	90.33
6.25	493.5	40.63	7.941	91.51
12.5	799.7	49.75	4.002	94.76

Table 8. Isotherms parameters for Adsorption of SH extract on steel X70 surface in HCl solution by weight loss, polarization, and EIS methods.

Methods	Isotherm	Equation	R^2	"a" or "g"
Weight loss	Langmuir	$c/\theta = 1.029c + 0.365$	0.998	1.029
	Temkin	$\text{Log}(\theta/c) = 3.750\theta + 2.466$	0.979	3.750
	Frumkin	$\text{Log}(\theta/(1-\theta)c) = -1.773\theta + 1.790$	0.742	-1.773
Polarization	Langmuir	$c/\theta = 1.015c + 0.172$	0.999	1.015
	Temkin	$\text{Log}(\theta/c) = 6.077\theta + 4.919$	0.960	6.077
	Frumkin	$\text{Log}(\theta/(1-\theta)c) = -2.059\theta + 2.468$	0.598	-2.059
EIS	Langmuir	$c/\theta = 1.045c + 0.190$	0.999	1.045
	Temkin	$\text{Log}(\theta/c) = 4.847\theta + 3.626$	0.936	4.847
	Frumkin	$\text{Log}(\theta/(1-\theta)c) = -2.255\theta + 2.352$	0.923	-2.255

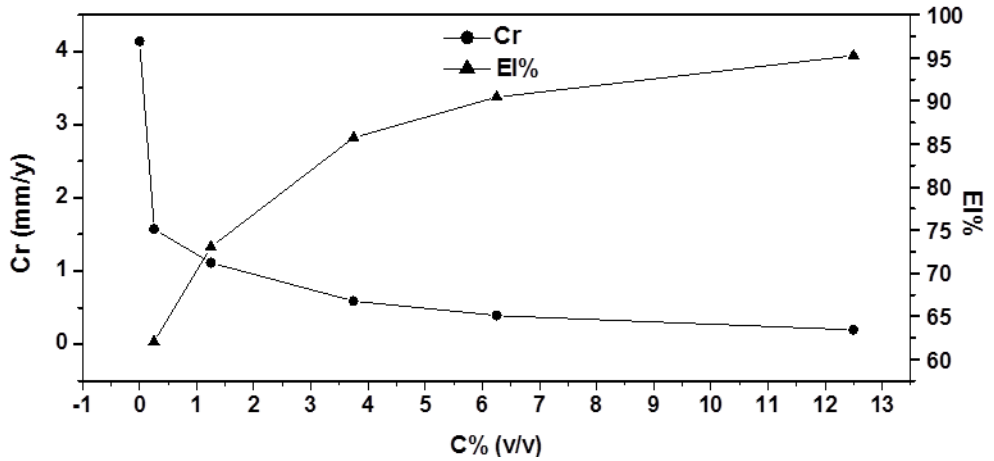

Figure 1. Variations of corrosion speed and inhibition efficiency of corrosion of carbon steel in 1M HCl with various concentrations of SH extract

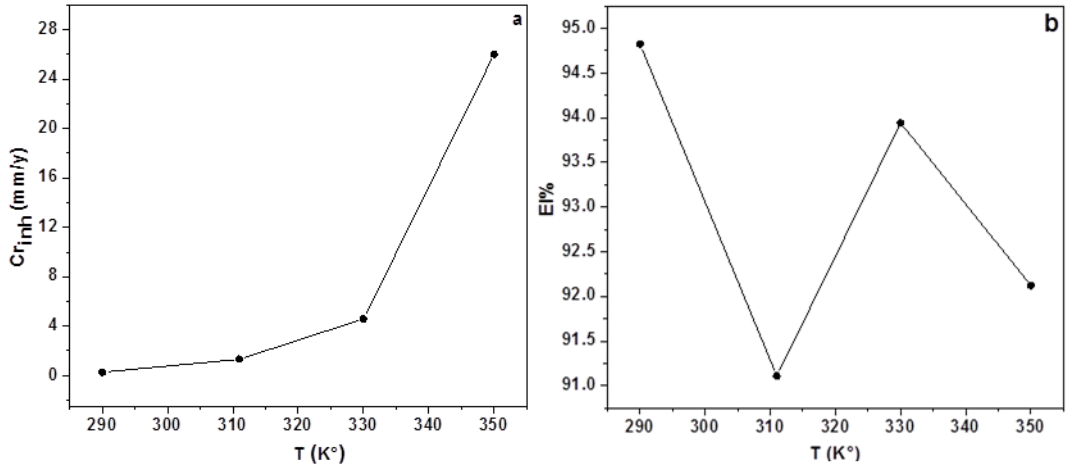

Figure 2. Effect of various temperatures on (a) the corrosion speed and (b) inhibition efficiency of carbon steel in 1M HCl in the existence 12.5% (v/v) of inhibitor

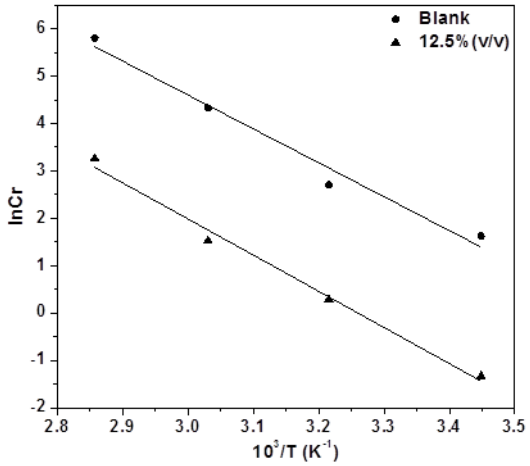

Figure 3. Arrhenius plots for the corrosion speed of carbon steel in 1M HCl in non-attendance and attendance of inhibitor

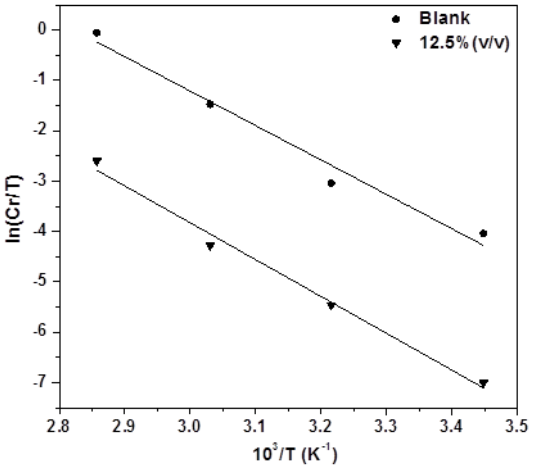

Figure 4. Transition state plot for the corrosion rate of carbon steel in 1M HCl in non-attendance and attendance of inhibitor

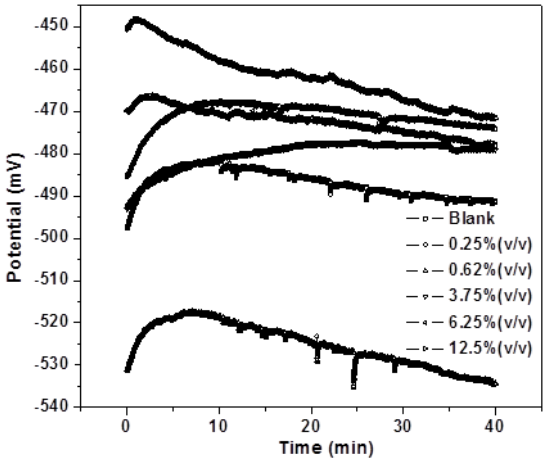

Figure 5. Variation of OCP with a time of carbon steel in non-attendance and attendance of various concentrations of inhibitor in 1M HCl solution.

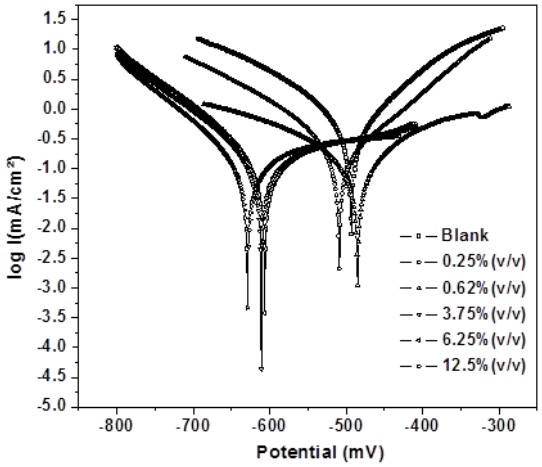

Figure 6. Potentiodynamic polarization curves for carbon steel in 1M HCl including various concentrations of SH extract.

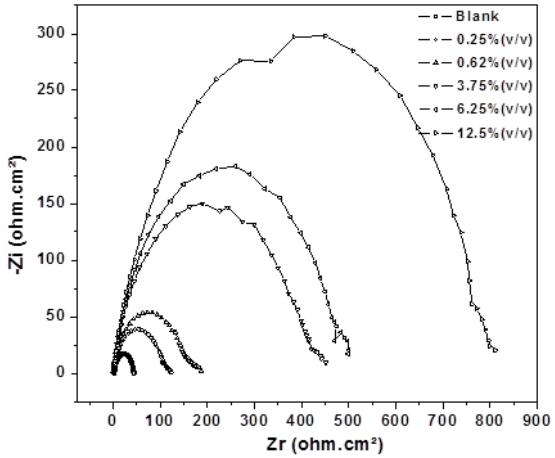

Figure 7. Nyquist diagrams for carbon steel in 1M HCl solutions in non-attendance and attendance various concentrations of SH extract.

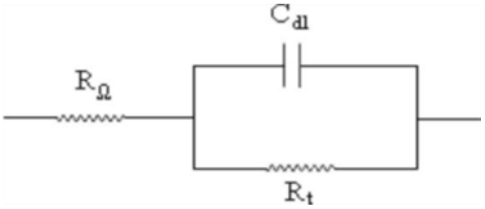

Figure 8. The electrical equivalent circuit model used to fit the EIS spectra

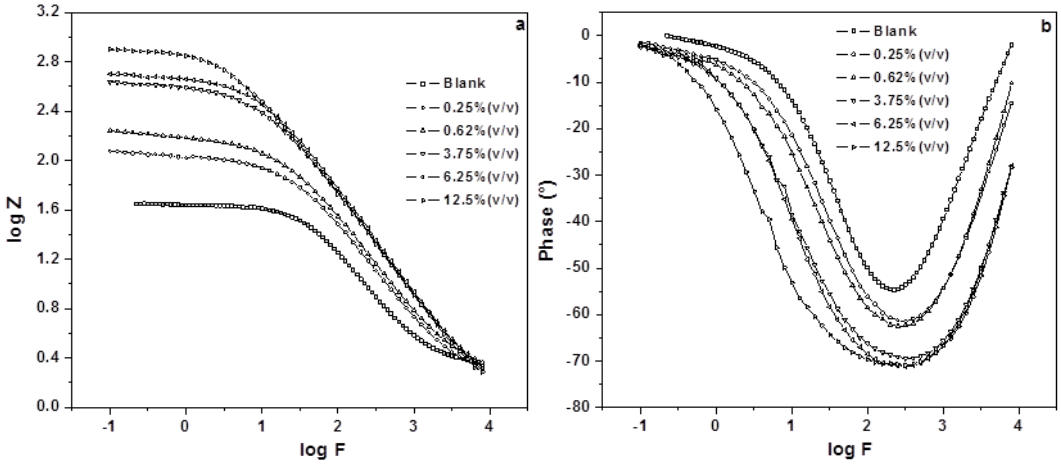

Figure 9. (a) Bode and (b) phase angle plots of carbon steel in 1M HCl in non-attendance and attendance various concentrations of SH extract.

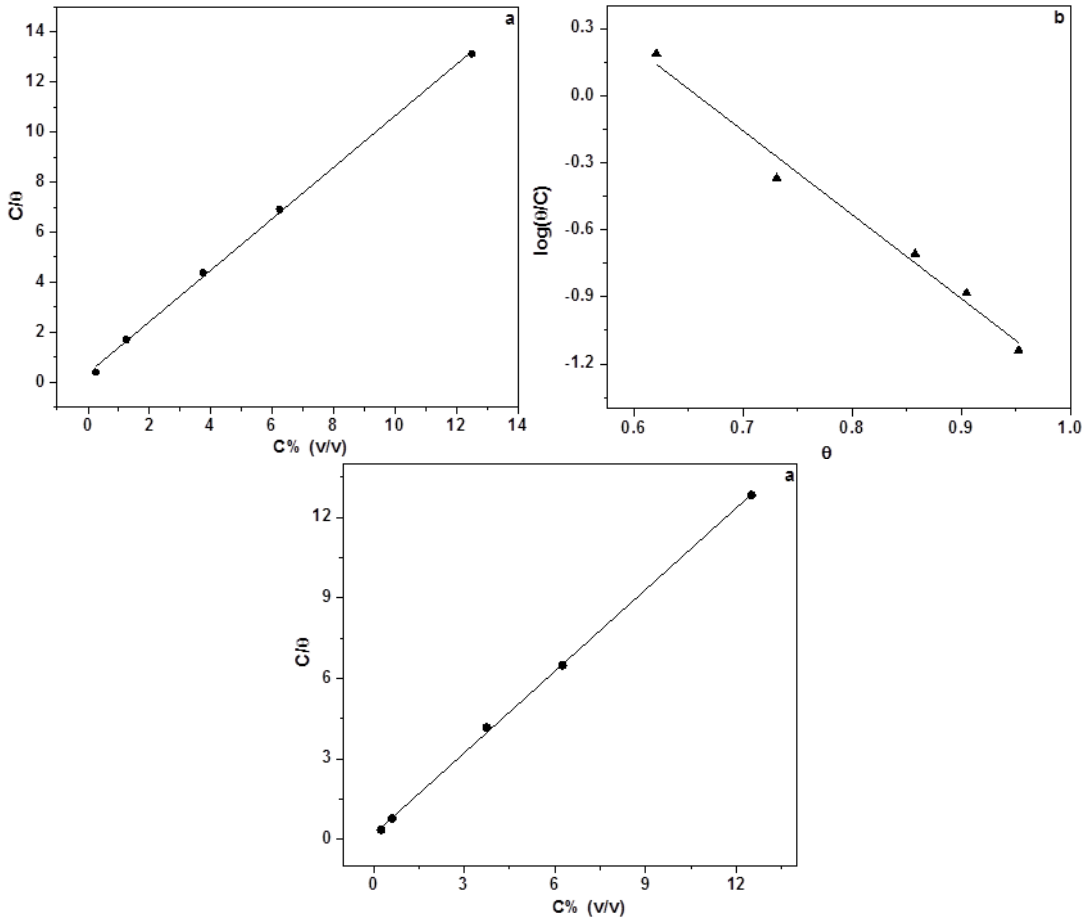

Figure 10. (a) Langmuir, (b) Temkin and (c) Frumkin isotherms for the adsorption of SH extract on the roof of steel X70 in HCl solution by weight loss method

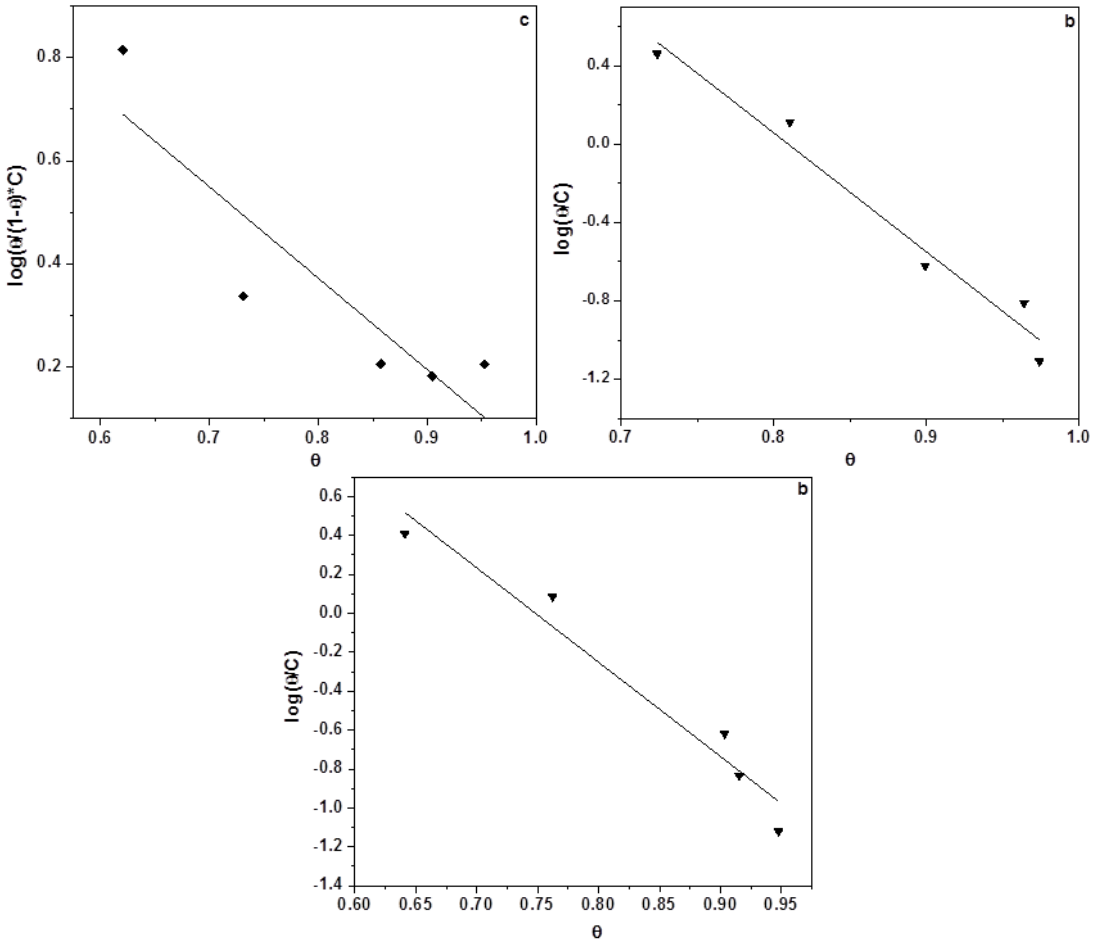

Figure 11. (a) Langmuir, (b) Temkin and (c) Frumkin isotherms for the adsorption of SH extract on the roof of steel X70 in HCl solution by polarization method

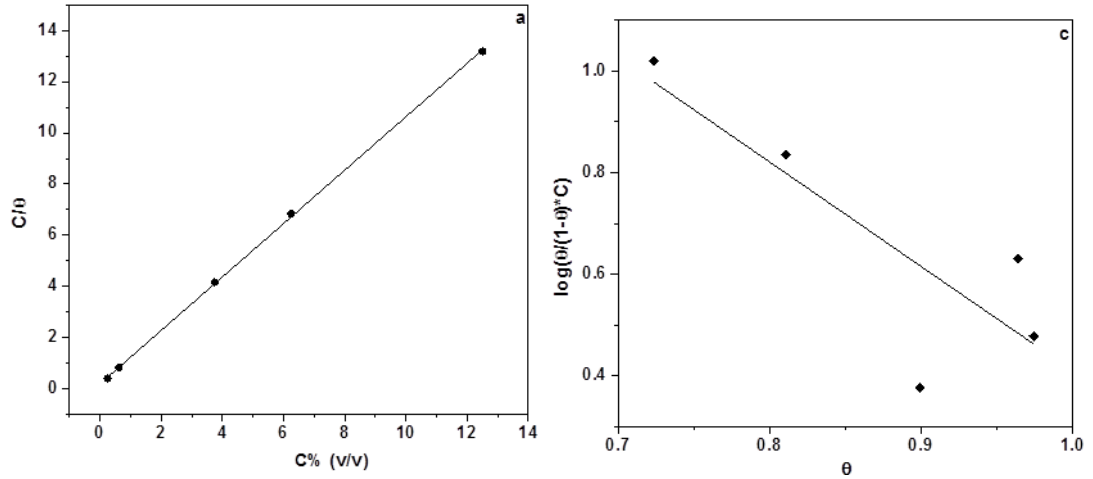

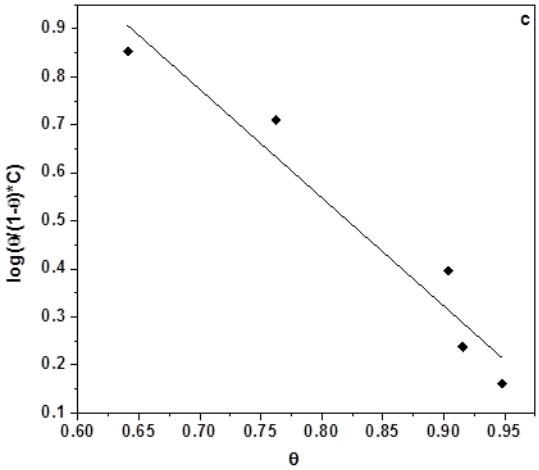

Figure 12. (a) Langmuir, (b) Temkin and (c) Frumkin isotherms for the adsorption of SH extract on the roof of steel X70 in HCl solution by EIS method
Note: All Curves were drawn by OriginPro 8

Conclusion

1) The weight loss, polarization, and EIS tests indicated that SH extract acted as a good protector of carbon steel from corrosion in 1 M HCl solution. This can be imputed to the fact that it contained chemical compounds that were adsorbed on the area of the metal.
2) The inhibition efficacy raised with the increased concentration of the inhibitor while it shown a decrease with increasing temperature.
3) The thermodynamic results confirmed that the process of adsorption of the plant extract particles on the surface of steel was of the physical type and endothermic.
4) Adsorption of green inhibitor on the surface of the metal obeys Langmuir adsorption isotherm.

References

[1] A.I. Ali, Y.S. Mahrous. (2017). Corrosion inhibition of c-steel in acidic media from fruiting bodies of *Melia azedarach L* extract and a synergistic Ni^{2+} additive. RSC Adv 7. 23687-23698.
[2] A.S. Fouda, H. Ibrahim, M. Atef. (2017). Adsorption and inhibitive properties of sildenafil (Viagra) for zinc in hydrochloric acid solution. Results in Physics 7. 3408-3418.
[3] D. Tahar, H. Hanane, D. Djamel. (2017). Effect of temperature and hydrodynamic conditions on corrosion inhibition of an azomethine compounds for mild steel in 1 M HCl solution. Journal of the Taiwan Institute of Chemical Engineers 71. 388-404.
[4] M.S. Al-Otaibi, A.M. Al-Mayouf, M. Khan. (2014). Corrosion inhibitory action of some plant extracts on the corrosion of mild steel in acidic media. Arabian Journal of Chemistry 7. 340-346.
[5] B. Evrim, C. Ahmet, Y. Birgul. (2016). Inhibitory effect of *Gentiana olivieri* extracts on the corrosion of mild steel in 0.5 M HCl: electrochemical and phytochemical evaluation. Arabian Journal of Chemistry: 1-17.
[6] C.D.R. Janaina, A.D.C.P.G. José, D.E. Eliane. (2010). Corrosion inhibition of carbon steel in hydrochloric acid solution by fruit peel aqueous extracts. Corrosion Science .52. 2341–2348.
[7] K.V. Dakeshwar, K. Fahmida. (2016). Green approach to corrosion inhibition of mild steel in hydrochloric acid medium using extract of spirogyra algae. Green Chemistry Letters and Reviews 9. 52–60.
[8] B.M.A. Muhamath, K. Kulanthai. (2009). Inhibition effect of *Parthenium hystophrous l* extracts on the corrosion of mild steel in sulphuric acid. J Appl Sci Environ Manage. 13. 27-36.
[9] N. Gherraf, Y.N. Tidjani, L. Segni. (2009). Aqueous extract of *Zygophyllum album* as corrosion inhibitor for mild steel in sulphuric acid medium. Am Eurasian J Sustain Agric. 3. 781-783.
[10] S. Rajendran, M. Agasta, R.B. Devi. (2009). Corrosion inhibition by an aqueous extract of Henna leaves (*Lawsonia Inermis* L). Journal Materials Protection Numbers 50. 77-84.
[11] P.B. Raja, A.A. Rahim, H. Osman. (2010). Inhibitory effect of *Kopsia singapurensis* extract on the corrosion behavior of mild steel in acid media. Acta Phys Chim Sin. 26. 2171-2176.
[12] K.O. Orubite, N.C. Oforka. (2004). Corrosion inhibition of zinc on HCl using *Nypa fruticans wurmb* extract and 1,5 diphenyl carbazone. J Appl Sci Environ Mgt. 8. 57-61.
[13] Z. Ghazi, H. ELmssellem, M. Ramdani. (2014). Corrosion inhibition by naturally occurring substance containing *Opuntia ficus indica* extract

on the corrosion of steel in hydrochloric acid. Journal of Chemical and Pharmaceutical Research. 6. 1417-1425.

[14] F. Haddouchi, T.M. Chaouche, N. Halla. (2016). Screening phytochimique, activités antioxydantes et pouvoir hémolytique de quatre plantes sahariennes d'Algérie. Phytothérapie. 1-9.

[15] S.J. Majid, A.H. Aya, Y.Y. Nahi. (2016). Detection of active compounds in the aqueous extract of the plant leaves for *Eriobotrya japonica* and study the effect of the extract as an antioxidant. Journal of Engineering and Technology 6. 204-208.

[16] S Ambrish, V.K. Singh, M.A. Quraishi. (2010). Effect of fruit extracts of some environmentally benign green corrosion inhibitors on corrosion of mild steel in hydrochloric acid solution. Mater Environ Sci 3. 162-174.

[17] M. Allaoui, O. Rahim, L. Sekhri. (2017). Electrochemical study on corrosion inhibition of iron in acidic medium by *Moringa oleifera* extract. Orient J Chem 33. 637-646.

[18] M. Allaoui, N. Gherraf, O. Rahim. (2017). Corrosion inhibition of carbon steel in 1M HCl medium using butanol extract of *Traganum nudatum* del.. International Journal of Applied Engineering Research 12. 6769-6777.

[19] A.I. Caroline, A.S. Abdul rahaman, I.H. Kobe. (2015). Inhibitive performance of bitter leaf root extract on mild steel corrosion in sulfuric acid solution. American Journal of Materials Engineering and Technology. 3. 35-45.

[20] B.E.A. Rani, B.B.J. Basu. (2012). Green inhibitors for corrosion protection of metals and alloys: an overview. International Journal of Corrosion. 1-15.

[21] S.A. Umoren, U.M. Eduok, M.M. Solomon. (2016) Corrosion inhibition by leaves and stem extracts of *Sida acuta* for mild steel in 1M H_2SO_4 solutions investigated by chemical and spectroscopic techniques. Arabian Journal of Chemistry 9. 209-224.

[22] M. Benahmed, I. Selatnia, A. Achouri. (2015). Steel corrosion inhibition by *Bupleurum lancifolium* (Apiaceae) extract in acid solution. Trans Indian Inst Met. 68: 393-401.

[23] M. Manssouri, Y. El Ouadi, M. Znini. (2015). Adsorption proprieties and inhibition of mild steel corrosion in HCl solution by the essential oil from fruit of Moroccan *Ammodaucus leucotrichus*. Mater Environ Sci 6. 631-646.

[24] S.O. Adejo, S.G. Yiase, U.J. Ahile. (2013). Inhibitory effect and adsorption parameters of extract of leaves *of Portulaca oleracea* of corrosion of aluminium in H_2SO_4 solution. Arch Appl Sci Res. 5. 25-32.

[25] M. Lebrini, F. Robert, C. Roos. (2013). Adsorption properties and inhibition of C38 steel corrosion in hydrochloric solution by some indole derivates: temperature effect, activation energies, and thermodynamics of adsorption. International Journal of Corrosion. 1-14.

[26] K.V. Dakeshwar, K. Fahmida. (2015). Corrosion inhibition of mild steel by extract of *Bryophyllum pinnatum* leaves in acidic solution. Chemistry and Materials Research 7. 69-76.

[27] N.M. Guan, L. Xueming, L. Fei. (2004). Synergistic inhibition between *o*-phenanthroline and chloride ion on cold rolled steel corrosion in phosphoric acid. Materials Chemistry and Physics. 86. 59-68.

[28] A. Singh, V.K. Singh, M.A. Quraishi. (2010). Aqueous extract of kalmegh (*Andrographis paniculata*) leaves asgreen inhibitor for mild steel in hydrochloric acid solution. International Journal of Corrosion. 1-11.

[29] M. Sanja, S. Ivica. (2002). Thermodynamic characterization of metal dissolution and inhibitor adsorption processes in the low carbon steel/mimosa tannin/sulfuric acid system. Applied Surface Science. 199. 83-89.

[30] A. Hamdy, N.S. El-Gendy. (2013). Thermodynamic, adsorption and electrochemical studies for corrosion inhibition of carbon steel by henna extract in acid medium. Egyptian Journal of Petroleum. 22. 17-25.

[31] A.A. Ganash. (2018). Theoretical and experimental studies of dried marjoram leaves extract as green inhibitor for corrosion protection of steel substrate in acidic solution. Chemical Engineering Communications. 205. 1-46.

[32] X. Xihua, S. Ambrish, S. Zhipeng. (2017). Theoretical, thermodynamic and electrochemical analysis of biotin drug as an impending corrosion inhibitor for mild steel in 15% hydrochloric acid. R Soc open sci. 4. 1-19.

[33] M.A. Migahed. (2005). Corrosion inhibition of steel pipelines in oil fields by N,N-di(poly oxy ethylene) amino propyl lauryl amide. Progress in Organic Coatings. 54. 91–98.

[34] K.V. Dakeshwar, K. Fahmida. (2016). Electrochemical study of corrosion inhibition of mild steel in hydrochloric acid solution by the extract of *Cuscuta reflexa*. Chemistry and Materials Research. 8. 1-7.

[35] Z. Yang, G. Lei, Z. Shengtao. (2017) Corrosion control of mild steel in 0.1 M H_2SO_4 solution by benzimidazole and its derivatives: an experimental and theoretical study. RSC Adv. 7. 23961-23969.

[36] S. Garima, B.V. Chandra, E.E. Ebenso. (2015). Thermodynamic and electrochemical investigation of (9-[(R) 2[[bis [[(isopropoxycarbonyl)oxy]methoxy] phosphinyl] methoxy] propyl] adenine fumarate) as green corrosion inhibitor for mild steel in 1M HCl. Int J Electrochem Sci. 10.1102-1116.

[37] H. Serrar, M. Larouj, H.L. Gaz. (2018). Experimental and theoretical studies of the corrosion inhibition of 4-amino-2-(4-chlorophenyl)-8-(2, 3-dimethoxyphenyl)-6-oxo-2, 6-dihydropyrimido [2, 1-b][1, 3] thiazine-3,7-dicarbonitrile on carbon steel in a 1.0 M HCl solution. Portugaliae Electrochimica Acta. 36. 35-52.

[38] M. Punita, B. Sitashree, M.M. Singh. (2014). Corrosion inhibition of mild steel in acidic solution by *Tagetes erecta* (Marigold flower) extract as a green inhibitor. Corrosion Science. 85. 352-363.

[39] S. Andreani, M. Znini, J. Paolini. (2016). Study of corrosion inhibition for mild steel in hydrochloric acid solution by *Limbarda crithmoides* (l.) essential oil of corsica. J Mater Environ Sci. 7. 187-195.

[40] M.H. Hussin, M.J. Kassim. (2011). The corrosion inhibition and adsorption behavior of *Uncaria gambir* extract on mild steel in 1M HCl. Materials Chemistry and Physics. 125. 461–468.

[41] M.M. Ihebrodike, A.U. Anthony, B.O. Kelechukwu. (2010). The inhibitive effect of *Solanum melongena* l. leaf extract on the corrosion of aluminium in tetraoxosulphate (VI) acid. African Journal of Pure and Applied Chemistry. 4. 158-165.

[42] S.O. Adejo, M.M. Ekwenchi, J.U. Ahile. (2014). Resolution of adsorption characterisation ambiguity through the adejo-ekwenchi adsorption isotherm: a case study of leaf extract of *hyptis suaveolen* poit as green corrosion inhibitor of corrosion of mild steel in 2M HCL. Journal of Emerging Trends in Engineering and Applied Sciences. 5. 201-205.

[43] S.O. Adejo, M.M. Ekwenchib, J.A. Gbertyoa. (2014). Determination of adsorption isotherm model best fit for methanol leaf extract of *Securinega virosa* as corrosion inhibitor for corrosion of mild steel in HCl. Journal of Advances in Chemistry. 10. 2737-2742.

[44] H. Mirghasem, F.L.M. Stijn, R.A. Mohammed. (2003). Synergism and antagonism in mild steel corrosion inhibition by sodium dodecyl benzenesulphonate and hexamethylenetetramine. Corrosion Science. 45. 1473–1489.

[45] E. Hassan, l. Khadija, S. Mostapha. (2015). Adsorption and inhibitive properties of tetradecyl triméthylammonium chloride for the corrosion of carbon steel in acid sulfuric. International Journal of Latest Trends in Engineering and Technology. 6. 423-434.